J. Membrane Biol. 24, 281–304 (1975)

Noise Measurements in Squid Axon Membrane

Harvey M. Fishman, Denis J.M. Poussart, and L.E. Moore

Department of Physiology and Biophysics, University of Texas Medical Branch, Galveston, Texas 77550,
Département de Génie Electrique et Centre de Recherches en Bionique, Université Laval, Québec, Canada and Marine Biological Laboratory, Woods Hole, Massachusetts 02543,
Department of Physiology, Case Western Reserve University School of Medicine, Cleveland, Ohio 44106

Received 10 March 1975

Summary. A small area (10^{-4} to 10^{-5} cm^2 patch) of the external surface of a squid (*Loligo pealei*) axon was "isolated" electrically by means of a pair of concentric glass pipettes and sucrose solution to achieve a low extraneous noise measurement of spontaneous fluctuations in membrane potential and current. The measured "small-signal" impedance function of the isolated patch in seawater was constant at low frequencies and declined monotonically at frequencies beyond 100 Hz. It is shown that the power-density spectrum (PDS) of voltage noise, which generally reflects the current-noise spectrum filtered by the membrane impedance function, is equivalent to the power spectrum of current-noise up to frequencies where the impedance decline is significant (Fishman, 1973*a*, *Proc. Nat. Acad. Sci. USA* **70**:876). This result is in contrast to an impedance resonance measured under uniform constant-current (internal axial wire) conditions, for which the voltage-noise PDS reflects the impedance resonance. The overdamped resonance in the patch technique is a consequence of the relatively low resistance (1 MΩ) pathways through the sucrose solution in the interstitial Schwann cell space which surround and shunt the high resistance (10–100 MΩ) membrane patch. Current-noise measurements during patch voltage clamp extend observation of patch ion-conductance fluctuations to 1 kHz. Various tests are presented to demonstrate the temporal and spatial adequacy of patch potential control during current-noise measurements.

In the application of kinetic methods to physical-chemical processes, several experimental techniques have been developed which enable determination of the critical parameters describing a chemical reaction (*cf.* Weissberger, 1963). Eigen and co-workers (1963) have used a variety of perturbation methods in which an equilibrated system is subjected to a sudden change in a single parameter, and the subsequent relaxation times of concentration changes are measured as the system returns to equilibrium. A particularly successful example of a perturbation method applied to biological membranes is the voltage-clamp technique of Cole (1949, 1968) which led to the Hodgkin and Huxley (1952) formalism. A combination of voltage-clamp technique and laser-induced temperature

jump has been applied directly to axon membrane (Moore, Holt & Lindley, 1972).

Recently, a new approach to chemical reaction kinetics, "fluctuation spectroscopy," was demonstrated for an electrolytic system (Feher & Weissman, 1973). This technique relies on the spectral analysis of spontaneous fluctuations from a system which is in macroscopic chemical equilibrium. The kinetic information which can be obtained from relaxation methods can also be obtained from the frequency spectrum. Consequently, fluctuation spectroscopy is of special importance to ion conduction in biological membranes since it can provide kinetic data without unduly perturbing the system. In some instances, such microscopic information may allow discrimination between conduction models (Hill & Chen, 1972; Stevens, 1972; Chen & Hill, 1973). In a preliminary publication (Fishman, 1973*a*), electrical noise associated with potassium-ion conduction in squid axon membrane was reported. The present communication describes the noise-measurement techniques and presents, in addition, tests of these measurements. A subsequent paper (Fishman, Moore & Poussart, 1975) presents noise data which relate to potassium-ion conduction.

Materials and Methods

Axon Preparation and Chamber

Giant axons from live squid, *Loligo pealei,* were used. They were obtained from May through September in four consecutive summers (1971–1974) at the Marine Biological Laboratory, Woods Hole, Mass. The axons ranged in size from 1080 μ (May) to 320 μ (July). Two axons were removed from each animal under flowing seawater and kept in a Petri dish at 8 °C. In a separate operation just prior to an experiment connective tissue was removed along a 3 mm length with the aid of a microscope (20–50 ×) and dark-field illumination. The details of these procedures have recently been described (Rosenberg, 1973). The axon rested on a Silgard (Dow Corning, Midland, Michigan) transparent pad (Fig. 1) and extended out of open sides of the chamber (Fishman, 1970) through air gaps (5 mm), on each side of the chamber, onto posts. The purpose of the pad was to prevent axon movement during the patch isolation procedure. Entry of internal perfusion pipette and electrodes into the axon was at the posts. The air gaps provided isolation of the axon in the chamber from the axon at the posts, and were the only means of electrical isolation in axial-wire experiments. External solution entered the chamber via an inlet hole 5 mm from the axon on the chamber floor and exited via two holes in which suction polyethylene tubes were placed to maintain a steady solution-level above the axon. The exit holes were located near the outer side edges of the chamber so that solution flow from inlet to exit tubes formed a triangular section. Most of the axon in the chamber was in this flow zone. Because of direct suction and surface tension, no chamber sides were necessary and a solution volume of 5 ml was maintained. On the inlet side of the axon a mirror tilted at 45° was placed

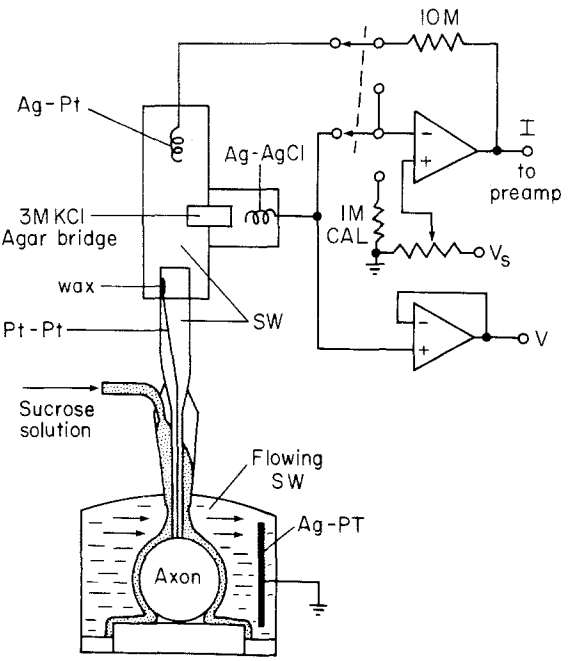

Fig. 1. Diagram of patch isolation technique and voltage clamp used to measure membrane current noise

for viewing the axon in the vertical plane from a microscope above. Two fiberlites mounted beneath the chamber provided cool, noise-free illumination of the axon.

Solutions

The standard external solution was filtered Woods Hole seawater (SW). In experiments in which the external solution composition was varied, artificial seawater (ASW: 430 mM NaCl, 5 mM KCl, 10 mM $CaCl_2$, 50 mM $MgCl_2$, 5 mM Tris-HCl) was used as the control solution. In experiments involving internal perfusion of axons, the standard perfusate was 0.5 M KF buffered to pH 7.4 at 25 °C with Tris-HCl. In some experiments pronase (approximately 0.1 mg/ml) was included initially in the perfusate for 2–3 min. This short treatment facilitated axoplasm clearance without any measurable effects on membrane characteristics. The method of internal perfusion used has been described previously (Fishman, 1970). Isosmotic sucrose-solution (0.8 M) was used for patch isolations (Stämpfli, 1954; Julian, Moore & Goldman, 1962). The conductivity of the sucrose solution relative to glass distilled water was checked to assure good isolations. When necessary, the sucrose solution was passed through an ion-exchange column.

Temperature Control and Monitor

Temperature of the external solution was lowered below ambient by passage through tubing immersed in an ice-water bath. Changes in flow rate were used to change solution temperature. Steady-state temperatures fluctuated less than ± 0.2 °C under these conditions.

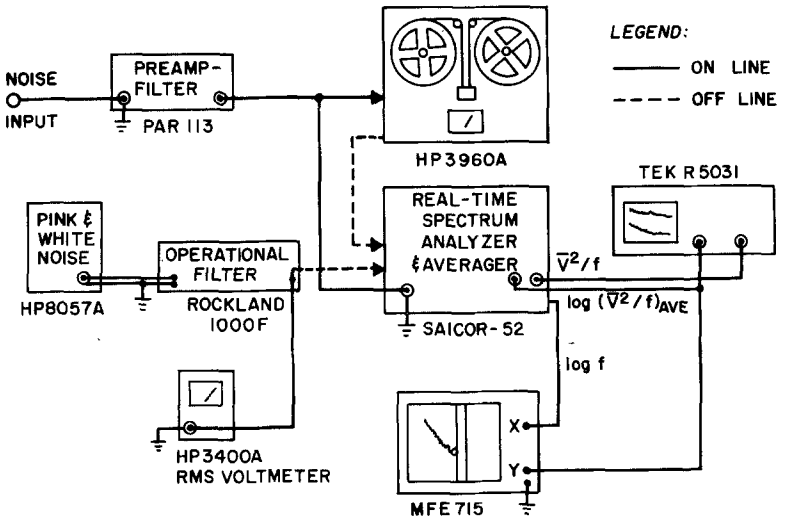

Fig. 2. Noise analysis and calibration instrumentation

The time required to change the temperature depended on the flow rate. The longest time to reach a steady-state condition was 5–10 min. Although other methods were contemplated, the ice-bath was judged to be simple, adequate, and, most importantly, noise-free. Temperature was monitored by a YSI model 73TE (Yellow Spring Instruments, Yellow Spring, Ohio) and 402 thermistor probe placed in the solution inlet to the chamber. Placement of the probe in the solution directly over the axon and along its length indicated, under all flow conditions, a maximum temperature difference of 1 °C from the values obtained at the inlet.

Electrostatic Shielding and Vibration Isolation

The chamber, perfusion solutions, ice bath, microscope, noise preamplifier and voltage-clamp circuitry were within a rectangular metal cage which provided effective electrostatic shielding of external sources of electric field. Noise induced by magnetic fields was not significant, and thus required no preventive measures. The power for the voltage-clamp system as well as the other instruments used to record, process, and analyze the acquired signals was acquired from an AC line source. The noise "signal" preamplifier (Fig. 2), however, was battery operated to eliminate ground-loop and common-mode signal problems.

Attenuation of floor vibrations was achieved by mounting the cage on a heavy platform which rested on four air-inflated tire inner tubes.

Instrumentation Noise and Selection of Membrane Area

Optimal measurement conditions for observation of membrane electrical noise depend upon minimizing extraneous sources of noise from (1) electrodes and access resistances to the membrane surfaces, (2) preamplifier, (3) mechanical vibrations, and (4) electromagnetic fields and common ground return paths in series with the preamplifier input terminals. Points (3) and (4) were reduced as described above. In addition, the resolution of the spectrum

analyzer (discussed in a later section) relaxed the need for more complex methods of eliminating or attenuating these sources. Vibrational and line-related spectral components occurred as discrete spectral lines in the overall spectra (Fig. 7) and were easily removed without significantly altering spectral shape. The major extraneous noise problems arise from (1) and (2).

Low-noise amplifiers usually have noise figures, NF, of less than 1 db. The lowest noise figures in the frequency range 1–1000 Hz are presently obtained from amplifiers with junction field-effect-transistor (JFET) input stages. However, low NF operation is attained only when the signal source-resistance equals the optimum noise-resistance of the amplifier (p. 35, Motchenbacher & Fitchen, 1973). The primary amplifier used in voltage-noise experiments was a PAR model 113 (Princeton Applied Research Corp., Princeton, N.J.) which achieves low noise operation, from 1 Hz to 1 kHz, when driven from megohm source resistances (Fig. 1, Fishman & Dorset, 1973). In general, in order to take advantage of the low NF of any FET amplifier, 1–10 megohm source resistances are required (*see* Appendix II,[1] Motchenbacher & Fitchen, 1973). Thus it is desirable to select a patch of membrane with impedance which properly matches the optimum range of the amplifier. With readily available technology and without resorting to special techniques such as cross-correlation (Poussart, 1973) this means (assuming a membrane resistance of 1000 Ωcm^2 for squid axon) the isolation of a small area, about 10^{-3} to 10^{-4} cm^2. The desirability of small area also applies to measurements of current fluctuations during voltage clamp (discussed in a later section) since the clamp must be capable of responding to patch voltage fluctuations in order to correct for the fluctuations and maintain a constant voltage condition.

Patch Electrode

The method chosen to record fluctuations from membrane patches is described in detail elsewhere (Fishman, 1975*b*). Briefly, two drawn glass capillaries are assembled in a coaxial configuration (Fig. 1). The inner pipette is filled with seawater and makes contact with the external axon surface. The outer capillary is used to direct the flow of isosmotic sucrose-solution (Stämpfli, 1954) over the region of axon surrounding the area underneath the aperture of the inner pipette. Measurements (Fishman, 1975*b*) indicated isolation resistances of 1–2 MΩ. The patch areas fulfilled the required value to achieve minimum noise from the PAR 113 or other FET amplifiers. In addition, the inner pipette had a floating platinized-platinum wire (25 μ diameter) within its length which produced a combined electrode and series resistance (100 kΩ) to the patch which was negligible compared to the resting patch resistance (10–100 MΩ) (Fishman, 1973*b*, 1975*b*).

Transpatch Rest Potential and Polarization

The electrical isolation of a small patch of membrane provides for good matching to the characteristics of low noise amplifiers. Patch isolation also obviates the need for a potential electrode within the axon, which enhances both axon survival and the chance of success with internal perfusion. Thus the apparent patch-potential V_{ap} which was measured in most instances, was the voltage between the inner pipette and chamber ground electrode

1 Appendix II contains noise data on six types of JFET. In particular, the frequency spectrum of intrinsic voltage e_n and current i_n noise of each device is given. From the ratio e_n/i_n the optimum noise-resistance can be calculated at each frequency. Generally these resistances range between 1 and 10 MΩ in the band 10–1000 Hz.

(Fig. 1). V_{ap} should reflect only *changes* from the absolute rest-potential since both the inner pipette and chamber ground are outside the axon. During a patch isolation with sucrose solution, V_{ap} was usually +20 to +30 mV, which is indicative of a resting hyperpolarization. To measure and compare absolute transpatch-potential with V_{ap}, an internal potential-sensing electrode (Fishman, 1973*b*) was introduced axially (Fishman, 1975*b*). Measurements with the internal electrode showed that V_{ap} in a resting patch (designated "rest" potential, 0 mV in all Figs.) was indeed hyperpolarized (corresponding to absolute transmembrane potentials of −80 to −90 mV) during isolation with sucrose in contrast to the normal potential (−60 mV) without sucrose solution flow. Membrane hyperpolarization due to the use of sucrose solution for isolation is known (Julian *et al.*, 1962).

Changes in V_{ap} about "rest" were made by applying constant current (through a 10 MΩ molded metal-film resistor) during voltage-fluctuation measurements. In voltage clamp, the patch was held at the "rest" value of V_{ap} in the quiescent state, which was determined operationally as the potential for zero mean patch-current. Changes in V_{ap} were made by changing the d–c command V_s to the clamp amplifier (Fig. 1). In all of the Figures the potentials indicated are displacements from "rest" with positive potentials corresponding to depolarization and negative to hyperpolarization.

Noise Analysis

The instrumentation used for analysis of membrane-patch current fluctuations, under conditions of low noise voltage clamp (next section), was the same as for voltage fluctuations except that the input signal to the PAR113 (Fig. 2) was the output of the operational amplifier in Fig. 1. The PAR 113 was used as a single-ended preamplifier with a low-frequency cutoff (0.01 to 0.1 Hz) in order to exclude extraneous d–c and long-term drifts from the spectral analysis. The high-frequency cutoff was 300 kHz. After preamplification of the noise waveform, the signal was recorded on FM magnetic tape (HP 3960A) for later spectral analysis and processed simultaneously by a real-time spectrum analyzer and averager (Honeywell-SAICOR model 52, Hauppauge, New York) in order to monitor spectral content in a selected frequency band during an experiment. The SAI-52 is a hybrid instrument which combines digital and analog processing techniques to produce a 400 point frequency spectrum in 8 analysis band every 160 msec. The speed and resolution is achieved by a time compression of the input signal. Briefly, the signal is filtered[2] to prevent "aliasing," converted to digital form (9 bit resolution), and placed in a circulating memory. The digitized waveform is then "read out" of memory at a fast rate and converted back to analog form which time compresses or translates all of the frequency components in the signal to high frequencies. The "speeded up" version of the original signal is then rapidly sequenced through a narrow band-pass high-frequency filter from which the spectral components are detected and available as a linear, log, or squared magnitude presentation versus frequency. In addition, a digital averager section, which increases statistical accuracy, allows the average of a selected number of real-time spectra to be displayed as a linear, log, or log of the squared magnitude presentation. The specific instrument used was modified to display log frequency so that an averaged power-density spectrum (PDS) $S(f)$, i.e., $\log \overline{|\Delta X|^2}/\Delta f$ *vs.* $\log f$ where X is voltage or current and f is frequency and the bar indicates average, could be obtained directly. These spectra were monitored on an oscilloscope and could be plotted on an X-Y recorder. To assess the SAI-52 capabilities in analyzing random noise signals, a noise generator (Hewlett-Packard model 8057A, Palo Alto, Ca.) was used to apply "white" and "pink" noise through an operational filter (Rockland model 1000F, West Nyack, New York) with specific passband characteristics. For example, Fig. 3 contains four generated

2 A six-pole low-pass filter with cutoff at 1/3 the sample frequency in each analysis band.

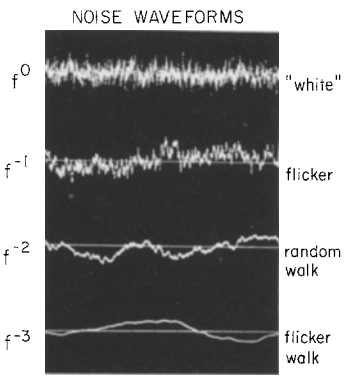

Fig. 3. Generated noise waveforms (by instrumentation in Fig. 2) with specific spectral distribution used to calibrate noise analysis system. White (f^0) and pink (f^{-1}) noise were available directly from the noise generator. f^{-2} and f^{-3} noises were produced by passing white and pink noise through a low-pass single pole filter with a corner frequency at 1 Hz

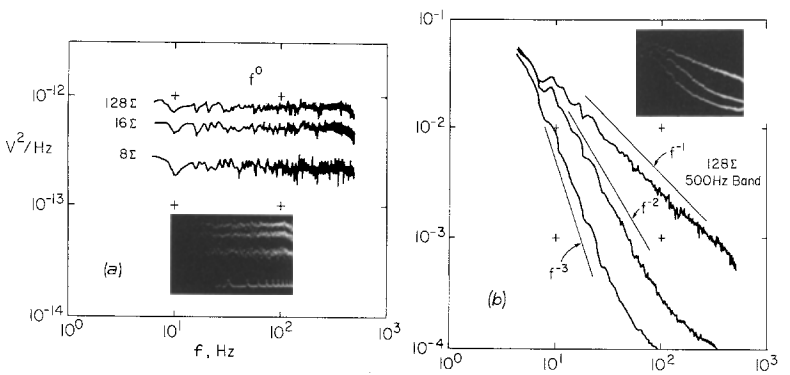

Fig. 4. (*a*) Power density spectra (PDS) in a 500 Hz band produced by averages (Σ) of a number of "real-time" spectra for "white" noise (f^0 distribution). (*b*) Same as (*a*) for noises with f^{-1}, f^{-2}, and f^{-3} spectral distributions. Inset shows 400 point spectra on an oscilloscope to compare with the "smoothed" reproductions produced by X-Y recorder

fluctuation waveforms: (1) "white" noise, $S(f)=K$ (constant), (2) "pink" or flicker noise, $S(f)=f^{-1}$, (3) "random walk," $S(f)=f^{-2}$, and (4) "flicker walk," $S(f)=f^{-3}$. Fig. 4 shows the results of the analysis of the average of 8, 16, and 128 real-time spectra in the 500 Hz analysis band as displayed on an oscilloscope and plotted on an X-Y recorder. The minimum distinguishable difference between two white-noise power levels was determined to be 12% for 128 averaged spectra. Fig. 4*b* shows the average of 128 spectra of the other waveforms in Fig. 3. Notice that the slopes of the actual spectra follow closely the drawn curves except at amplitudes below the dynamic range of the instrument (25 db in power). Analysis of frequency components which fall below the dynamic range requires further signal amplification.

The noise characteristics of the PAR 113 were measured by terminating the input with various resistors. These data were presented previously (Fig. 1, Fishman & Dorset, 1973).

Measurements of minimum distinguishable differences in thermal level between two resistors terminating the PAR 113 input were also made. The change in thermal noise produced by a 12% change of resistance at 1 MΩ was distinguishable in power spectra.

Low Noise Voltage Clamp

A single FET-input operational amplifier (Analog Devices model 43K, Norwood, Mass.) was used to apply, to the patch, clamp potentials which were derived from a Hg battery. The output voltage of the amplifier (Fig. 1) is proportional to the patch current and contains current-fluctuation information. The large feedback resistor (10 MΩ) assures good "signal-to-noise" ratio (Poussart, 1971, Appendix). This point is demonstrated in Fig. 5*a*. The current-noise power spectrum from a 1 MΩ resistor used as a thermal-noise source was measured by the clamp amplifier (shown in inset of Fig. 5*a*) with different feedback resistors R_{fb}. The thermal noise was computed from the Nyquist relation and is the dashed line. The noise figure of the measurement circuit is defined as 10 log of the ratio of total noise power output (referred to the input) to thermal noise of the source (1 MΩ). The deviation of the measured power spectrum from the dashed line in Fig. 5*a* is therefore the NF of the measurement circuit. With an R_{fb} of 10 MΩ, the NF over the entire frequency range is

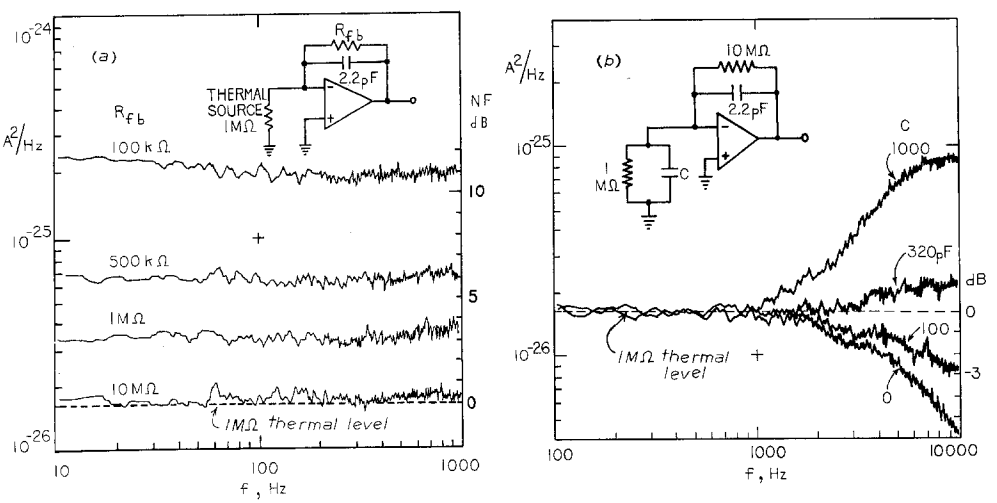

Fig. 5. (*a*) Measurement of the noise characteristics of the clamp amplifier with a constant 1 MΩ thermal noise source (equivalent to patch source resistance) at its input and the effect of variation of feedback resistance R_{fb}. The deviation from the thermal power density is a measure of the noise figure, NF, of the amplifier. Low NF is obtained only when the ratio of R_{fb}-to-source R is 10:1 (Poussart, 1971). (*b*) High frequency noise characteristics of clamp amplifier in (*a*) with and without a capacitive reactance to simulate membrane capacitance, in parallel with a 1 MΩ thermal noise course. The intrinsic voltage noise of the amplifier produces a frequency-dependent current noise through the source capacitance which becomes apparent beyond 1 kHz with increasing C. Patch capacitance was measured to be $\leqq$100 pF (Fishman, 1975*b*) and thus low extraneous current-noise measurements can be made to about 2 kHz. The 2.2 pF feedback capacitor was required for a nonpeaking "roll-off" in amplifier response

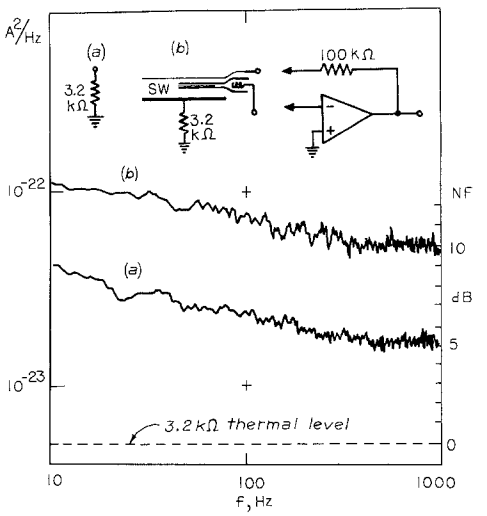

Fig. 6. (*a*) Measurement of the noise characteristics of the clamp amplifier with a 3.2 kΩ thermal source (equivalent to resistance of membrane in axial-wire clamp measurement). Both terminals of the clamp amplifier were connected to the top of the 3.2 kΩ resistor. (*b*) The same measurement as in (*a*) but with the clamp amplifier connected to the terminals of the "piggyback" electrode which was in a SW bath. Another bath electrode was connected in series with a 3.2 kΩ resistor to ground. This latter configuration measures extraneous noise from both electrodes and the amplifier terminated in the equivalent source resistance of the axon. FET amplifiers have relatively poor NF when driven from low source resistances. Noise from the potential-sensing electrode is also emphasized

a few tenths of a db. Reduction of R_{fb} to 1 MΩ yields a NF of 3 db and further reduction results in substantial degradation of NF as indicated by Poussart (1971). In Fig. 6, curve (*a*), the same FET operational amplifier was used but with a source resistance of 3.2 kΩ and a R_{fb} of 100 kΩ. Although the ratio of R_{fb}-to-source resistance exceeds 10:1, a large NF in the frequency band is obtained. These measurements serve to illustrate that an FET-input amplifier provides excellent signal/noise performance only if the source resistance is in the MΩ range, and R_{fb} is relatively higher. Thus the choice of a 1 MΩ patch of membrane for noise measurements follows. The selection of R_{fb} as 10 MΩ is a compromise between low noise performance and good frequency response, which are achieved at the expense of one another. For example, Fig. 5*b* (C=0) shows the frequency response of the clamp circuit with a 1 MΩ thermal source and 10 MΩ R_{fb}. The response, with the 2.2 pF capacitor across R_{fb} for a nonpeaking "roll-off," is −3 db at 5 kHz which is adequate for noise measurements to 1 kHz. The response could be increased by lowering R_{fb}. However, as indicated in Fig. 5*a*, a reduction in R_{fb} below 10 MΩ degrades noise performance. Alternatively, an increase in R_{fb} above 10 MΩ would produce a reduction in NF (although not significantly), but it would also decrease frequency response and lower the noise measurement bandwidth to <1 kHz.

An additional complication in achieving low noise performance occurs at frequencies beyond 1 kHz when the source impedance contains a capacitive reactance component. The noise properties of an amplifier can usually be characterized by an equivalent voltage-noise source in series and an equivalent current-noise source in parallel with its input (Motchenbacher & Fitchen, 1973). Even if the contribution from these sources is small at low frequencies, if the source impedance contains a capacitive element, the amplifier voltage noise

will produce a current noise through the source capacitance which increases with frequency (*see* Poussart, 1971, Eq. 4A). Eventually, beyond some frequency, this extraneous current noise becomes "overpowering." As an example, Fig. 5*b* shows the effect of shunting the 1 MΩ thermal noise source with increasing values of capacitance. With an estimated patch capacitance of 100 pF or less, this effect becomes significant beyond 5 kHz.

Access Resistance

The total resistance between potential-control points which lead to inner and outer patch surfaces constitutes a resistance in series with membrane impedance. The access resistance can produce an error in steady-state potential across the membrane as well as other errors in a voltage clamp (Taylor, Moore & Cole, 1960). Access resistance was usually not compensated for two reasons:

(1) Compensation schemes require positive feedback which produces additional noise.

(2) Since "rest" potential is actually a hyperpolarized (20–30 mV) membrane (*see* previous section on rest potential), the maximum depolarizations made in these experiments, in fact, only moved the membrane potential back to the normal rest or to potentials only slightly depolarized from normal rest. Even for these maximum depolarizations, the membrane resistance remains relatively high, and the effect of access resistance is probably minimal (several Ω cm^2 compared to 1000 Ω cm^2) (Fishman, 1975*b*).

System Noise Test

The noise contribution of the measurement schemes in Figs. 1 and 2 was determined by isolating a patch of substitute membranes. Fig. 7 shows the results of one such measurement in which a rubber condom was placed over a bottle cap, which was cemented to the bottom of a bowl filled with seawater. The coaxial assembly was lowered onto the condom surface while monitoring the resistance from inner pipette to a Ag-Pt wire in the SW. When a slight increase in resistance was observed, the advance was stopped and sucrose solution flow was initiated through the outer pipette. In the example shown, the measured resistance reached a steady value of 1.5 MΩ. In contrast to an axon, the condom membrane is nonconducting and backed by air so that 1.5 MΩ is a measure of the isolation provided by the flowing sucrose solution. This value is comparable to the estimated isolation resistance obtained on axons. An analysis of fluctuations under these conditions should indicate all possible sources of extraneous noise. The contributions other than thermal noise are small over the frequency range 10–1000 Hz. Below 10 Hz, components which are 1–2 magnitudes above the thermal level occur. These are due, in part, to mechanical agitation of the condom by the flowing sucrose solution. This "vibrating drum" noise could be reduced by decreasing the area of the bottle cap over which the condom was spread. At frequencies beyond 1 kHz, the 1.5 MΩ source resistance together with the total input capacitance to the PAR 113 produced attenuation. The voltage-noise PDS shown is a composite reproduction of three overlapping analysis bands, which are indicated by arrows on the frequency axis. Line-related components at 60 and 180 Hz and a vibrational component at 3.6 Hz occur in this spectrum and serve to illustrate that the analyzer resolution permits graphical removal of such components without distorting the overall spectrum. Additional checks of system voltage and current noise were made on patches of air bubbles in SW (Fishman, 1975*b*). Essentially the same spectrum (Fig. 7) was obtained as with the condom.

Tests were made on the isolated condom patch (Fig. 7) to establish that noise artifacts were not produced as a result of polarization effects from the long-term (minutes) application of current or voltage to the patch electrode. No changes in spectra were observed for prolonged

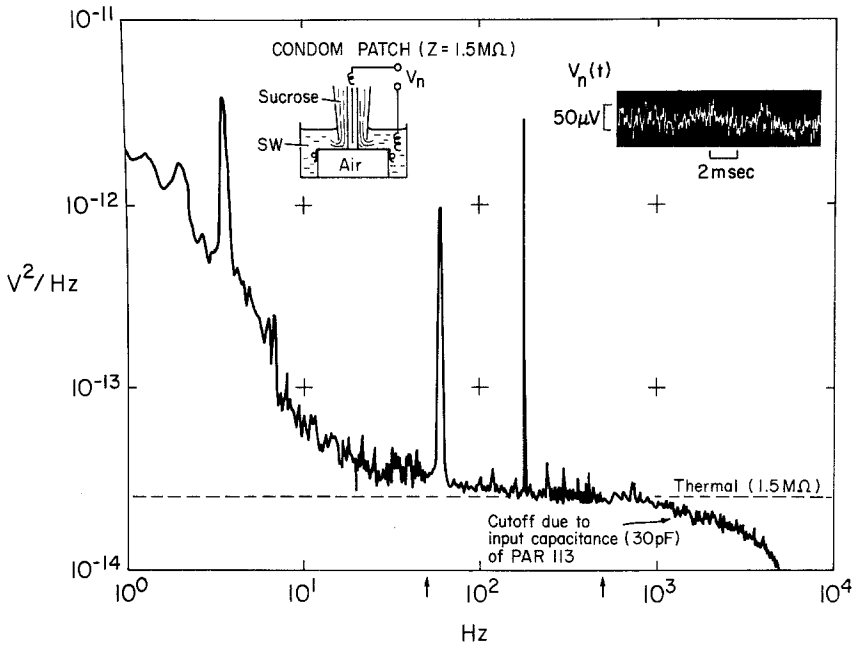

Fig. 7. Measurement of extraneous voltage noise contributed by the entire patch measurement system. A condom placed over a bottle cap (inset) was used as a substitute impermeable membrane, and a patch was "isolated" from the SW bath after sucrose solution flow. The deviation from the thermal noise spectrum corresponding to the isolation resistance (1.5 MΩ) is extraneous noise. Current noise under voltage clamp gave a spectrum similar in form to the voltage noise PDS. The PDS in this figure is a composite reproduction from three overlapping analysis bands, delimited by arrows on the frequency axis. The discrete frequency components at 3.6, 60, and 180 Hz relate to AC line and vibration and could not be eliminated entirely. The analyzer's resolution allows graphical removal without distortion of spectral form

applied polarizations. In addition, long time-records (data blocks) of fluctuations, which were tape recorded from axon patches, have been analyzed in different portions of a data block by reducing the number of real-time spectra averaged, thereby reducing analysis time. In all cases, the spectra show stationarity throughout the data block for analysis which is initiated at arbitrary points in time within each continuous data block.

Internal Axial Wire Measurements

Voltage and current noise and impedance were measured with internal electrodes from large areas of the same axon. A compound "piggyback" electrode (Fishman, 1970, 1973*b*) consisting of a long tapered potential pipette and a Pt-Pt wire mounted atop the pipette, and extending beyond the aperture of the pipette a distance the length of the axon in the chamber, was inserted axially into the axon. A Ag-Pt electrode was used as an external chamber ground. The axial-current wire was insulated with wax over the portion which was at the entry point into the axon. The air gaps (*see* Axon Preparation and Chamber) provided isolation of the axon membrane area from which potentials and currents were recorded. Generally, the area of membrane isolated using this method was very large (0.3 cm^2)

and is similar to the areas measured by Wanke, DeFelice and Conti (1974) with a similar external air-gap, internal axial-wire technique. The voltage-clamp circuit used for the patch technique (Fig. 1) was also used for axial-wire measurements with the feedback resistor of the clamp amplifier reduced to 100 kΩ. The noise from this system was considerably larger than for the patch technique due to the low source-impedance of the large membrane areas. Fig. 6 illustrates this point. The current noise of the clamp was measured with a 3.2 kΩ resistor substituted as a thermal source for the membrane. The NF ranges from 5–9 db in the 10–1000 Hz band. The low source-resistance of the large membrane area also emphasizes the voltage noise of the potential-sensing electrode, which was observed by clamping the SW bath through a 3.2 kΩ resistor to ground as indicated in the inset (*b*) of Fig. 6. The measured NF of 10–13 db demonstrates the relatively high extraneous noise conditions which may result when measuring from large areas of membrane compared to the noise obtained from a small patch (Figs. 5, 7) measurement.[3]

Impedance Measurements

The magnitude of impedance of the membrane in both patch and axial wire techniques was measured by applying Gaussian white noise as a constant current to the membrane and recording the voltage response, which was spectrum analyzed. The magnitude of the impedance function which was measured in response to white noise as a stochastic signal was demonstrated to be equivalent to application of sinusoids of different frequency, one at a time, on lumped RC and RLC circuits and on the axon membrane as well. The amplitude of the current source was adjusted to keep the peak-to-peak voltage (noise or sinusoids) to less than 5 mV, for which the membrane behavior appeared to be linear.

Results

Comparison of Patch and Axial Wire Noise Measurements

In preliminary accounts of noise measurements (Fishman, 1973*a*, 1975*a*), it was stated that power spectra of spontaneous voltage fluctuations measured in the patch are essentially the same as spectra of spontaneous current fluctuations for low frequencies. At high frequencies (e.g., above several hundred Hz) membrane impedance filters voltage noise to produce a steeper decline. In general, since spontaneous fluctuations are low amplitude, for which linearity may be assumed, the PDS of voltage noise is equal to the product of the squared-magnitude of the impedance function and the PDS of current noise (Poussart, 1971; Stevens, 1972), that is,

$$S_V(f) = |Z(f)|^2 S_I(f) \tag{1}$$

3 Although desirable for space-clamp control, the use of external guard electrodes introduces a very low resistance (e.g., 10–50 ohms) shunt across the virtual ground of the current recording amplifier. Amplifier voltage noise across that shunt is reflected as large current noise, with considerable degradation of system noise performance. Therefore external guard electrodes were not used.

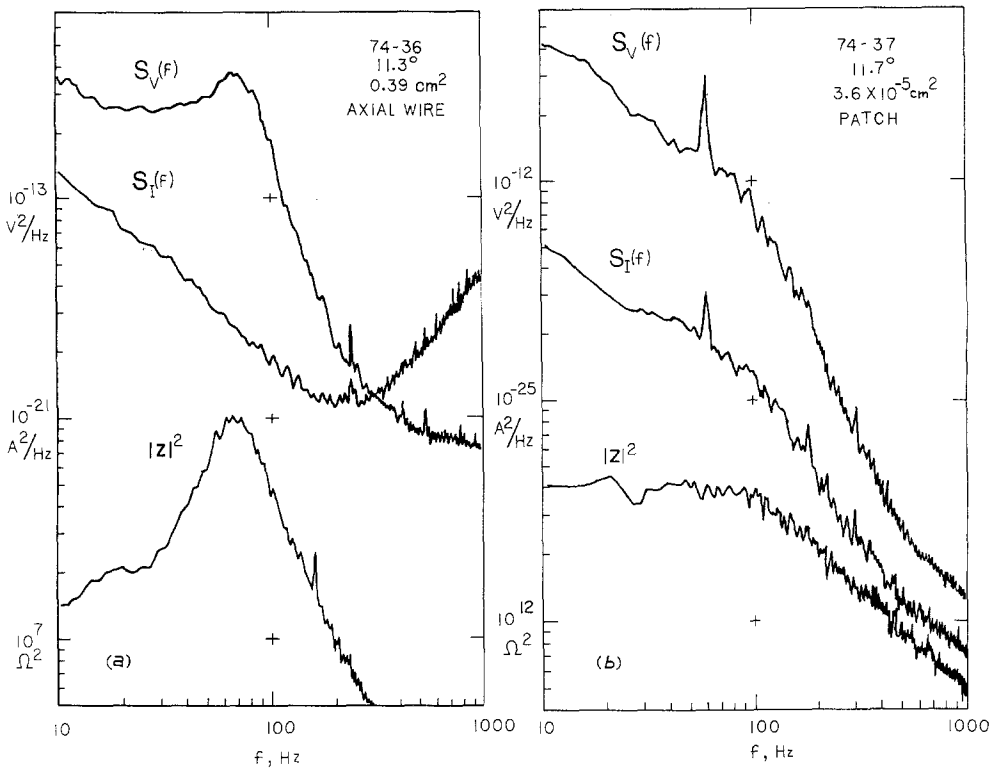

Fig. 8. (*a*) PDS of voltage noise $S_V(f)$, current noise $S_I(f)$, and the squared magnitude of impedance $|Z|^2$, spectrum measured from the same large area of membrane at rest potential with axial-wire technique. (*b*) The same measurements as in (*a*) from a small area of membrane with the patch technique. In (*a*) the impedance resonance is reflected in $S_V(f)$, whereas $S_I(f)$, which is the ratio of $S_V(f)/|Z(f)|^2$, shows only a $1/f$ decline and a high-frequency rise due to amplifier intrinsic voltage noise and the large membrane capacitance. In (*b*) the impedance resonance is overdamped; $|Z|^2$ is constant at low frequencies, and declines monotonically at high frequencies. At low frequencies, both $S_V(f)$ and $S_I(f)$ show a hump and are related by the constant $|Z|^2$; at high frequencies $S_V(f)$ declines more steeply than $S_I(f)$ due to the decline in $|Z|^2$. Patch PDS of voltage and current noise are thus equivalent at low frequencies whereas the impedance resonance in large membrane area measurements makes the form of the two spectra different

where $S_V(f)=\overline{|\Delta V|^2}/\Delta f$, $S_I(f)=\overline{|\Delta I|^2}/\Delta f$. It is evident from this relation that the impedance of the preparation will be reflected in PDS of voltage-noise. However, if the impedance function is constant over the frequency range of spectral analysis, voltage-noise PDS have the same form as current-noise PDS and are related by a constant scale factor.

It is well known that the small-signal impedance function of squid axon membrane shows resonance behavior (Cole, 1968; Conti, 1970; Mauro, Conti, Dodge & Schor, 1970). Consequently, the impedance

resonance should be reflected in power spectra of voltage fluctuations. Fig. 8*a* demonstrates this point. The squared-magnitude impedance function measured with internal axial-wire air-gap technique shows a prominent resonance at membrane rest-potential. The voltage-noise PDS from the same axon at rest, although different in form, shows peaking at the frequency of the impedance resonance. The measured current-noise PDS under voltage clamp, however, does not reflect the impedance resonance and shows approximately f^{-1} behavior out to frequencies where the clamp amplifier voltage-noise and membrane capacitance produce significant noise, as discussed previously.[4] The ratio of $S_V(f)/S_I(f)$ in Fig. 8*a* agrees reasonably well with the measured $|Z(f)|^2$. These results are in agreement with those reported by Wanke *et al.* (1974), using similar methods. However, conditions of the patch technique and the axial-wire air-gap technique are quite different. The difference is evident in the impedance function. Fig. 8*b* shows the same kind of data as obtained with axial wire, but with the patch technique. The squared-magnitude impedance measured at "rest" potential[5] shows no evidence of resonance but rather is constant at low frequencies and declines monotonically at frequencies beyond 100 Hz. The impedance resonance is completely damped out (overdamped) as a result of the relatively low resistance pathways through the sucrose solution which surround and shunt the high-resistance patch of membrane. The basis for this statement is the measured patch parameters (Fishman, 1975*b*). The patch capacitance, determined by integration of the charging current for a step voltage clamp, is 10–100 pF (depending upon diameter of inner pipette in contact with axon surface). For a 1 $\mu F/cm^2$ membrane (Cole, 1968), the patch area is in the range 10^{-4} to 10^{-5} cm^2. For a 1000 μ cm^2 membrane (Cole, 1968), the patch resistance range is 10^7 to $10^8\,\Omega$. Since the apparent patch resistance (patch resistance in parallel with shunt isolation resistance) is typically 1 MΩ, the ratio of patch resistance to shunt resistance is probably no less than 10:1. It can be demonstrated that a 10:1 ratio is more than adequate to damp the normal impedance resonance which occurs in squid axon under axial-wire conditions (Fishman, 1975*a*). Fig. 9*b* shows an impedance function measured by axial-wire technique and the effect on the measured impedance of

4 In a limited series of 10 axon experiments with axial-wire technique, relaxation spectral components could *not* be clearly distinguished from a general f^{-1} background. Sharply resonating impedance curves and other criteria (rest potential, spike amplitude) indicated that these axons were in good condition.

5 The absence of resonance in the patch is not due to a resting hyperpolarization since resonance was not observed for prolonged depolarizations to patch potentials which elicited spikes for short duration pulses.

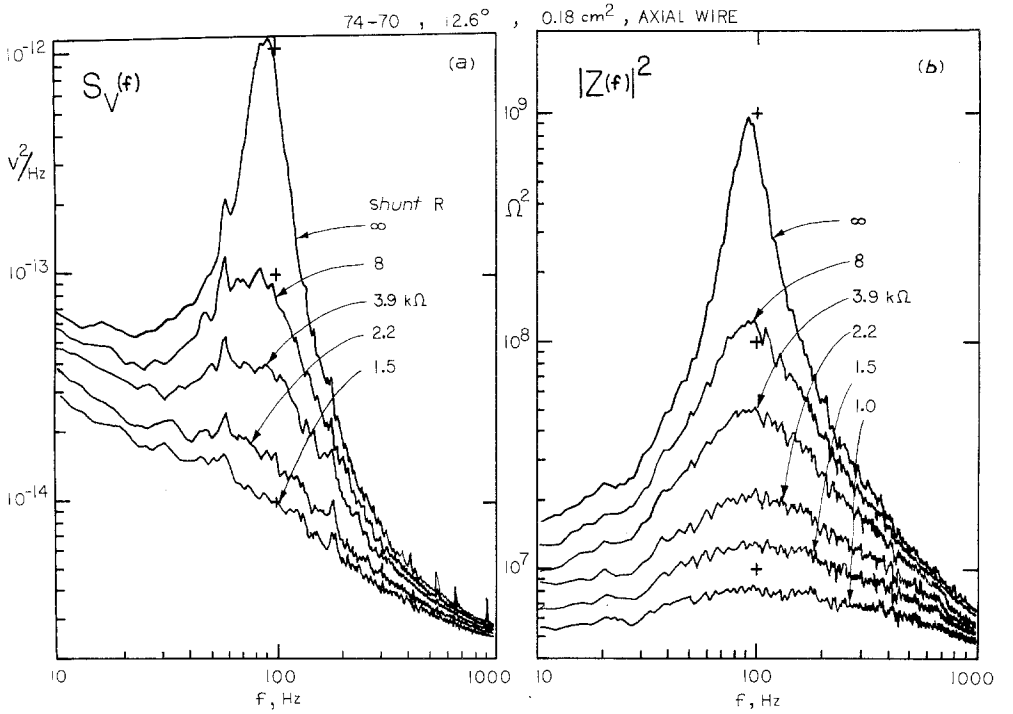

Fig. 9. PDS of voltage noise (*a*) and the squared magnitude of impedance (*b*) measured from the same membrane at rest potential with axial-wire technique and for various shunt resistors placed directly across the membrane (axial wire to ground). The resting resistance of this membrane was 4 kΩ and thus a ratio of membrane resistance-to-shunt resistance of $\geqq 5:1$ is sufficient to overdamp the resonance in impedance and $S_V(f)$. Compare $S_V(f)$ of 1.5 kΩ shunt spectrum, with $S_I(f)$ in Fig. 8*a*

connecting a lumped resistor from axial wire to ground, i.e., shunting the membrane impedance. A shunt resistance of 8 kΩ produces a significant effect on the impedance, and further decreases in the shunt resistance drastically damp the resonance. It should be noted that there was no change in rest potential or other conditions during these measurements. The measured resistance of this membrane was about 4 kΩ and thus a membrane resistance-to-shunt resistance of $\geqq 5:1$ appears adequate to effectively damp the resonance. In Fig. 9*a* the effect on voltage noise of shunting the same axon membrane is presented. The peaking in the voltage noise PDS diminishes as the impedance resonance becomes damped, and the spectrum with a 1.5 kΩ shunt resembles the current-noise PDS under voltage clamp shown in Fig. 8*a*. These data thus demonstrate that under axial-wire conditions, an impedance resonance does occur and is reflected in power spectra of spontaneous voltage fluctuations. However, the impedance resonance can be damped out by a shunt which is 1/5

the membrane resistance, in which case the impedance remains relatively constant over several hundred Hz and voltage and current-noise PDS are equivalent.

Returning to Fig. 8*b*, the equivalence of patch voltage and current-noise PDS, measured in the same patch as the $|Z|^2$ function (in the lower portion of the figure), show a pronounced hump superposed on a declining spectrum. The forms of these spectra are the same except at high frequencies where the voltage spectra decline more steeply as a consequence of the decline in $|Z|^2$. Nevertheless, the hump, which is a manifestation of a relaxation process (Fishman, 1973*a*, 1975*a*; Fishman *et al.*, 1975) in K^+ conductance, is evident in both patch voltage and current-noise PDS.

An estimate of patch area can be obtained by comparing current-noise power measured from the patch with the same data obtained by the axial-wire method. At 100 Hz in Fig. 8*a*, $S_I(f) = 1.8 \times 10^{-21}$ A^2/Hz measured from an area of 0.39 cm^2. $S_I(f)$ at 100 Hz, measured from a patch (Fig. 8*b*), is 10^{-25} A^2/Hz. The patch area calculated from these data is 2.2×10^{-5} cm^2 which agrees with estimates obtained from patch capacitance measurements (Fishman, 1975*a*).

In principle, then, whenever the small-signal impedance of a preparation is known and especially if it is relatively constant in the range of interest (as in the present patch method), useful information about conductance fluctuations can be extracted from voltage noise data. These considerations therefore reconcile criticism (Wanke *et al.*, 1974) of the interpretation of patch voltage noise measurements.

Finally, it should be noted that, even under idealized conditions (no instrumentation/electrode noise), all present voltage clamp systems are macroscopic, i.e., the gross transmembrane potential which the clamp attempts to maintain constant represents the superposition of a relatively large number of individual sources (presumed to be channels). Even if this is done successfully, there is no absolute assurance, presently, that the spontaneous field fluctuations, which might be expected to occur at the microscopic level of each of the sources, are effectively suppressed. This raises a question about the very meaning of "voltage clamp" itself with regard to noise measurements and inferences about underlying mechanisms.

Patch Voltage-Clamp Noise Measurements

Although patch voltage-noise PDS contain conductance information below several hundred Hz, analysis of current noise during voltage clamp

extends direct observation of conductance fluctuations to 1 kHz (Fig. 5). Since the patch voltage clamp technique employed here is relatively new, experiments designed to test its adequacy (consistent with the "signal" levels measured) with respect to temporal and spatial control of potential fluctuations across the patch are presented. The properties of this method which pertain to large-signal step-clamp currents are described elsewhere (Fishman, 1975*b*).

Control of Potential in Time

From the diagram (Fig. 1) of the patch electrode, the first obvious concern with respect to adequate clamping is the access resistance from the potential sensing electrode to the patch. The access path constitutes a resistance which is in series with the usual "series resistance" of a squid axon preparation. If the access is significant relative to the patch resistance, then aberrations, in addition to those associated with "series resistance" (Taylor *et al.*, 1960), will occur. Measurements of the equivalent resistance of this pipette with a Pt-Pt wire within its length have been described (Fishman, 1973*b*). With the inner pipette filled with SW and isolating a patch, an access resistance (pipette plus series) of 100 kΩ (7 Ω cm^2) or less was measured (Fishman, 1975*b*). From the previous measurements of patch capacitance (Fishman, 1975*b*), estimates of patch area, and the assumption of 1000 Ω cm^2 membrane at rest, the patch resistance is calculated to be 10^7 to 10^8 Ω. Consequently, the access resistance is apparently 2 to 3 orders of magnitude below the patch resistance and should not produce significant differences between the measured and actual potential across the patch.

As an independent check that the access resistance produces negligible error, a current-noise spectrum from a patch was obtained (Fig. 10, lower curve). The access resistance was then compensated by feedback as shown in the circuit of Fig. 10. The feedback was adjusted so that the compensation was greater than 50% but less than 90% of the access resistance. The resulting current-noise spectrum (Fig. 10, upper curve) is identical in form to that obtained without compensation. The overall increase in the power spectrum with compensation is due to the increased transfer gain[6] and additional noise arising from the positive feedback,

6 The transresistance (ratio of output voltage to input current) of this circuit is approximately $R_f/(1-\alpha)$, where R_f denotes the feedback resistance and α is the fraction of output voltage reinjected to the positive input terminal of the operational amplifier.

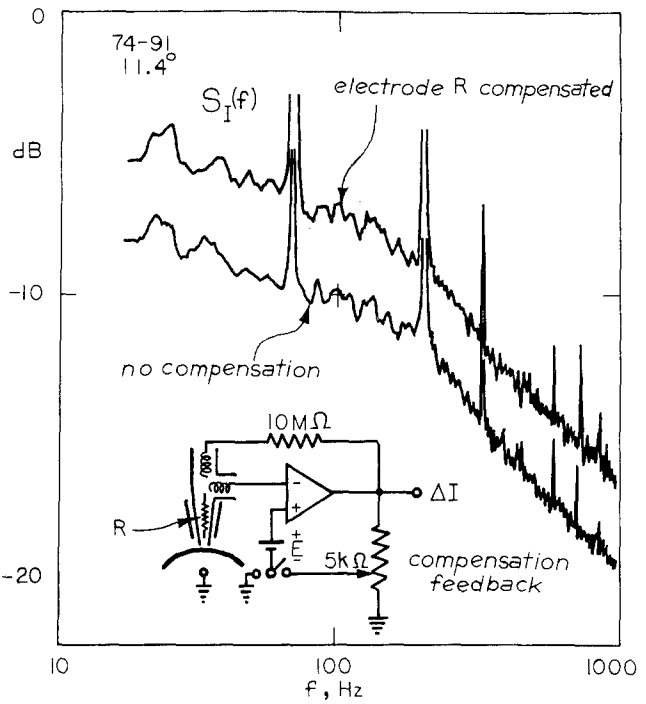

Fig. 10. Effect of compensation for access resistance to the patch on PDS of current noise under voltage clamp. Compensation was >50% but <90%. The form of the spectrum is unchanged and indicates that access R produces no significant error in clamping. Increase in overall noise power-density with compensation reflects an increase in gain and extraneous noise produced by positive feedback

as mentioned earlier in the section on access-resistance compensation. These data, therefore, suggest that the access resistance does not produce aberrations in the patch voltage-clamp measurement of current noise.

A stringent test of the adequacy of a voltage-clamp system with respect to its capability to maintain a constant potential over the frequency range of measurement is the degree to which membrane capacitance effects are removed. If a lumped capacitance is placed in shunt with the membrane, from Eq. (1) the voltage noise PDS will be altered because of the change in $|Z|^2$, whereas under voltage-clamp conditions the current-noise PDS should be unaltered by the added capacitance. Fig. 11 shows the result of this experiment wherein 0.002 μF (about 20 times patch capacitance) was placed in shunt with the patch. The added C affects the voltage noise by producing a spectrum decline earlier than without the added C. The current-noise spectra, however, with and without the added C are unchanged except at high frequencies. The increase in noise at high frequencies is expected due to the intrinsic voltage noise of the clamp amplifier

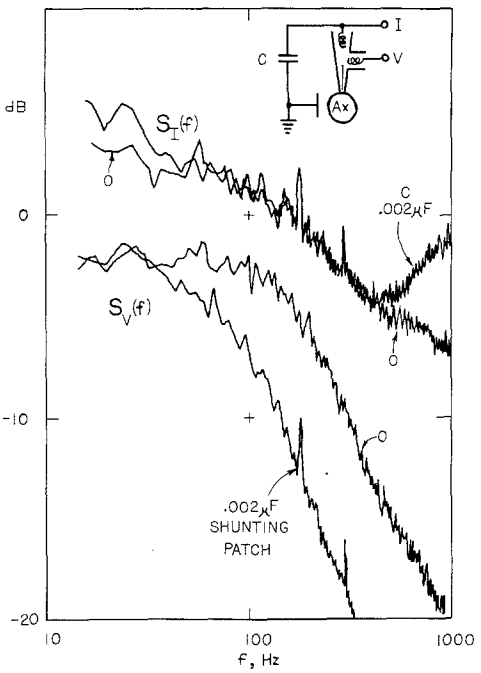

Fig. 11. Effectiveness of patch voltage clamp in removing capacitance in current-noise measurement. $S_V(f)$ and $S_I(f)$ were recorded from a patch with no added capacitance and with 0.002 μF (20× patch capacitance) shunting the patch. The added capacitance produces noticeable filtering in $S_V(f)$ as expected; however, it does not affect $S_I(f)$ except at high frequencies where the intrinsic voltage noise of the clamp amplifier appears due to the increased C

driving a current through the enhanced capacitance, and is evidence that the added capacitance is part of the patch measurement. This test strongly suggests that the patch voltage clamp is adequate for noise measurements in the frequency range of interest.

Spatial Control of Potential over the Patch

An additional constraint on a voltage-clamp technique is the maintenance of uniform potential control over the region of membrane from which current is measured. Since the isolated patch area is relatively small, favorable conditions for uniformity are expected. Nevertheless, this aspect has been investigated by measuring the potential with an independent internal axial pipette at various positions along the axon during step-voltage clamp of a patch. No difference was observed between the potential recorded by the internal voltage probe and the potential recorded via

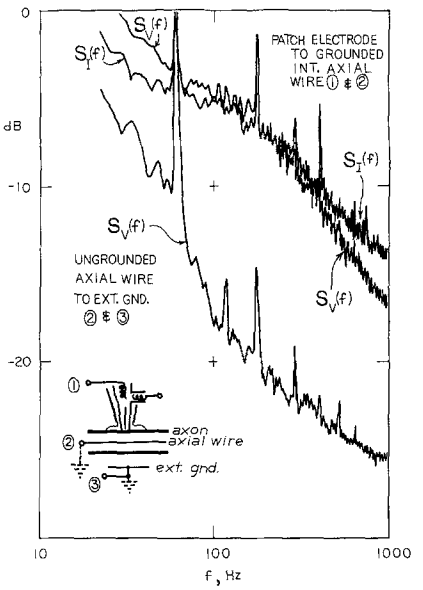

Fig. 12. Measurement of patch $S_V(f)$ and $S_I(f)$ with an internal axial wire (inset). Spectra were the same when measurements were made with respect to the external ground and no axial wire inside. In addition, $S_V(f)$ of voltage noise between internal axial wire and external ground shows insignificant noise contribution from axon membrane outside the patch

the patch electrode (Fishman, 1975*b*). In addition, patch noise measurements were made with a Pt-Pt axial wire as a ground within the axon while recording from a patch. Fig. 12 shows these data. Both patch voltage and current-noise PDS are the same, except for the high frequency decline, regardless of whether the return current path from the patch is through the internal axial-wire or through the rest of the axon membrane to an external electrode. The lowest curve in Fig. 12 shows the PDS of voltage noise recorded between the internal axial wire and the external electrode to be well below the noise from the patch. These data indicate clearly that the noise recorded from the patch is essentially from the patch and does not contain significant contributions from the remainder of axon membrane in the SW bath. Furthermore, the fact that noise spectra are the same with or without an internal "space" clamp (axial wire), although not conclusive, also suggests that the spatial clamp is adequate.

As a final test of the uniformity of potential over the patch, current-noise PDS were measured from a patch with SW in both the access pipette and in the surrounding bath. The chamber solution was then changed from SW to 0.5 M KCl (no Ca) while maintaining the same axon

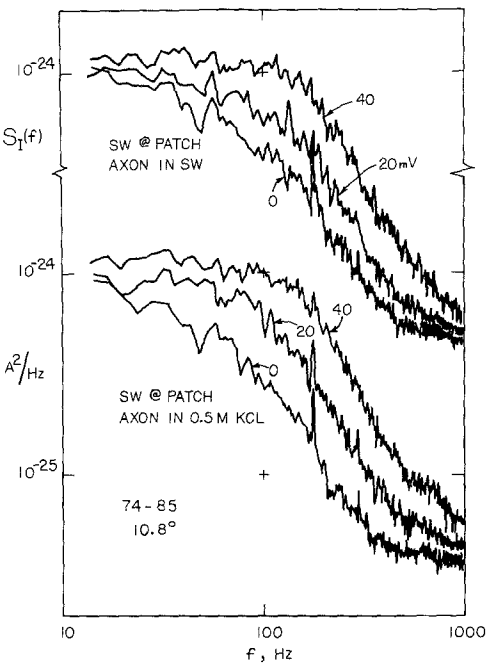

Fig. 13. Comparison of $S_I(f)$ of current noise for the same patch in SW at the designated depolarized potentials away from rest while the remainder of the axon was bathed either in SW or in 0.5 M KCl (axon rendered inexcitable). The similarity between spectra suggests negligible noise contribution and good spatial control of potential over axon membrane outside the patch

patch in SW. Twenty minutes after the external solution change, current-noise PDS were obtained for comparison (Fig. 13). Spikes could be elicited in the patch under all solution conditions,[7] whereas two axons with an internal axial wire showed no activity in the remainder of the axon externally perfused with the 0.5 M KCl solution. The 0.5 M KCl solution produces depolarization and subsequent inactivation of the Na^+ process; thus activity is abolished over the entire axon except at the patch. The two sets of spectra in Fig. 13 show reasonable agreement at "rest" and for polarizations of the patch. These data again support the assertion that good spatial control is obtained over the patch.

7 The maintenance of activity at the patch, while the remainder of the axon is rendered inactive, indicates exchange between the SW solution in the patch electrode and the access space to the patch as well as isolation from the external bath. The exchange could be further demonstrated by the reestablishment of activity in an isolated patch (SW in patch electrode) of membrane which had previously been externally bathed with 0.5 M KCl solution for 10 min and was inexitable.

Discussion

Measurement of steady-state fluctuations in potential and current from small patches of axon membrane show: (1) Nearly optimal (low) extraneous noise conditions in the frequency range 10–1000 Hz from both electrodes and instrumentation; (2) The normal "small-signal" impedance resonance which is measured from large areas of axon, under "space" clamp conditions, is completely damped (overdamped) by the "shunting" effect of the isolation medium on the patch impedance. The impedance is a constant at low frequencies ($\leqq 100$ Hz) and thus PDS of voltage noise are equivalent to PDS of current noise. Above 100 Hz the impedance declines monotonically and thus voltage-noise PDS reflect current-noise PDS which are "filtered" by the declining impedance function; (3) Current-noise measurements under voltage clamp remove the filtering action of the impedance and extend observations of conductance fluctuations to 1 kHz; (4) The access resistance to the patch does not produce significant aberrations in voltage clamping; (5) Test of the clamp's capability to eliminate the effect of capacitance on current noise indicates that it is effective for $20\times$ patch capacitance, and therefore the temporal characteristics of the clamp are adequate; (6) Spatial control of potential over the patch is demonstrated by the invariance of noise PDS with and without an internal axial wire and before and after the axon is rendered inactive in KCl solution.

These findings thus indicate that noise measurements of small membrane areas isolated by sucrose are self consistent and meet the usual criteria necessary for voltage-clamp measurements. An interesting feature of the patch technique is the similarity of the voltage and current-noise spectra which is a consequence of the severely damped impedance resonance by the sucrose shunt pathways. This situation is similar to the focal recording method used for end plate currents and noise measurements from the neuromuscular junction (Katz & Miledi, 1972). The focal recording method can be considered to be analogous to a voltage clamp in that the membrane current is being measured from a small membrane area under approximately constant potential while the voltage measurements made in the vicinity of the small area reflect the total membrane area with its impedance properties.

Ideally, it would be desirable to reduce the area still further and record single channel kinetics under voltage-clamp conditions; however, presently this does not appear possible in axon membranes due to an inability to isolate small enough areas and the presence of f^{-1} noise. Nevertheless,

the patch method appears to improve the channel noise resolution in comparison to large area axial-wire measurements. In our experience relaxation components were hardly detectable above the f^{-1} background in axial-wire measurements in axons which were in excellent condition.

Since single channels are not measured with either method, the question of whether or not a microscopic voltage clamp is possible must be considered. In both axial-wire space-clamped axons and voltage-clamped patches the potential control of a macroscopic system is achieved at essentially one point. This means that local variations at the individual channel sites could be quite large. If this is the case, then the form of current-noise spectra is complicated by an interaction with the total membrane impedance.

We thank Dr. Kenneth S. Cole for discussions and suggestions and Mr. William Law, Jr. for assistance in instrumentation. The work was supported in part by National Institutes of Health grants NS 09857 (H.M. Fishman), NS 11764 (H.M. Fishman) and NS 80409 (L.E. Moore); and Canadian National Research Council grant A5274 to D.J.M. Poussart. H.M. Fishman thanks the SUNY Research Foundation for awards during his affiliation with the Department of Biological Sciences, SUNY at Albany.

References

Chen, Y-D, Hill, T.L. 1973. Fluctuations and noise in kinetic systems. Application to K^+ channels in squid axon. *Biophys. J.* **13**:1276

Cole, K.S. 1949. Dynamic electrical characteristics of squid axon membrane. *Arch. Sci. Physiol.* **3**:253

Cole, K.S. 1968. Membrane Ions and Impulses. University of California Press, Berkeley

Conti, F. 1970. Nerve membrane electrical characteristics near the resting state. *Biophysik* **6**:257

Eigen, M., DeMaeyer, L. 1963. Relaxation methods. *In:* Techniques of Organic Chemistry. A. Weissberger, editor. Vol. 8, p. 895. Wiley-Interscience, New York

Feher, G., Weismann, M. 1973. Fluctuation spectroscopy: Determination of chemical reaction kinetics from the frequency spectrum of fluctuations. *Proc. Nat. Acad. Sci. USA* **70**:870

Fishman, H.M. 1970. Direct and rapid description of the individual ionic currents of squid axon membrane by range potential control. *Biophys. J.* **10**:799

Fishman, H.M. 1973*a*. Relaxation spectra of potassium channel noise from squid axon membranes. *Proc. Nat. Acad. Sci. USA* **70**:876

Fishman, H.M. 1973*b*. Low-impedance capillary electrode for wide-band recording of membrane potential in large axons. *IEEE Trans. BME* **20**:380

Fishman, H.M. 1975*a*. Noise measurements in axon membranes. *Fed. Proc.* **34**:1330

Fishman, H.M. 1975*b*. Patch voltage clamp of squid axon membrane. *J. Membrane Biol.* **24**:265

Fishman, H.M., Dorset, D.L. 1973. Comments on electrical fluctuations associated with active transport. *Biophys. J.* **13**:1339

Fishman, H.M., Moore, L.E. Poussart, D.J.M. 1975. Potassium-ion conduction noise in squid axon membrane. *J. Membrane Biol.* **24**:305

Hill, T.L., Chen, Y.-D. 1972. On the theory of ion transport across the nerve membrane. IV. Noise from the open-close kinetics of K^+ channels. *Biophys. J.* **12**:948

Hodgkin, A.L., Huxley, A.F. 1952. A quantitative description of membrane current and its application to conduction and excitation in nerve. *J. Physiol. (Lond.)* **117**:500

Julian, F.J., Moore, J.W., Goldman, D.E. 1962. Membrane potentials of the lobster giant axon obtained by use of the sucrose-gap technique. *J. Gen. Physiol.* **45**:1195

Katz, B., Miledi, R. 1972. The statistical nature of the acetylcholine potentials and its molecular components. *J. Physiol.* **224**:665

Mauro, A., Conti, F., Dodge, F., Schor, R. 1970. Subthreshold behavior and phenomenological impedance of the squid giant axon. *J. Gen. Physiol.* **55**:497

Moore, L.E., Holt, J.P., Lindley, B.D. 1972. Laser temperature-jump technique for relaxation studies of the ionic conductances in myelinated nerve fibers. *Biophys. J.* **12**:157

Motchenbacher, C.D., Fitchen, F.C. 1973. Low Noise Electronic Design. Wiley, New York

Poussart, D.J.M. 1971. Membrane current noise in lobster axon under voltage clamp. *Biophys. J.* **11**:211

Poussart, D.J.M. 1973. Low-level average power measurements: Noise figure improvements through parallel or series connection of noisy amplifiers. *Rev. Sci. Instrum.* **44**:1049

Rosenberg, P. 1973. The giant axon of the squid: A useful preparation for neurochemical and pharmacological studies. *In:* Methods of Neurochemistry. R. Fried, editor. Vol. 4, p. 97. Marcel Dekker, New York

Stämpfli, R. 1954. A new method for measuring membrane potentials with external electrodes. *Experientia* **10**:508

Stevens, C.F. 1972. Inferences about membrane properties from electrical noise measurements. *Biophys. J.* **12**:1028

Taylor, R.E., Moore, J.W., Cole, K.S. 1960. Analysis of certain errors in squid axon voltage clamp measurements. *Biophys. J.* **1**:161

Wanke, E., DeFelice, L.J., Conti, F. 1974. Voltage noise, current noise and impedance in space clamped squid giant axon. *Pflügers Arch.* **347**:63

Weissberger, A. (editor). 1963. Techniques of Organic Chemistry, Vol. 8. Interscience, New York